Inorg. Chem. **2005**, *44*, 8552–8560

Synthesis of the Pivalamidate-Bridged Pentanuclear Platinum(II,III) Linear Complexes with Pt···Pt Interactions

Kazuko Matsumoto,* Saiko Arai, Masahiko Ochiai, Wanzhi Chen, Ayako Nakata, Hiromi Nakai, and Shuhei Kinoshita

Department of Chemistry, Advanced Research Center for Science and Engineering, Waseda University, 3-4-1 Okubo, Shinjuku-ku, Tokyo 169-8555, Japan

Received June 10, 2005

Pentanuclear linear chain Pt(II,III) complexes $\{[Pt_2(NH_3)_2X_2((CH_3)_3CCONH)_2(CH_2COCH_3)]_2[PtX'_4]\}\cdot nCH_3COCH_3$ ($X = X' = Cl$, $n = 2$ (**1a**), $X = Cl$, $X' = Br$, $n = 1$ (**1b**), $X = Br$, $X' = Cl$, $n = 2$ (**1c**), $X = X' = Br$, $n = 1$ (**1d**)) composed of a monomeric Pt(II) complex sandwiched by two amidate-bridged Pt dimers were synthesized from the reaction of the acetonyl dinuclear Pt(III) complexes having equatorial halide ligands $[Pt_2(NH_3)_2X_2((CH_3)_3CCONH)_2(CH_2COCH_3)]X''$ ($X = Cl$ (**2a**), Br (**2b**), $X'' = NO_3^-$, $CH_3C_6H_4SO_3^-$, BF_4^-, PF_6^-, ClO_4^-), with $K_2[PtX'_4]$ ($X' = Cl$, Br). The X-ray structures of **1a**–**1d** show that the complexes have metal–metal bonded linear Pt_5 structures, and the oxidation state of the metals is approximately Pt(III)–Pt(III)···Pt(II)···Pt(III)–Pt(III). The Pt···Pt interactions between the dimer units and the monomer are due to the induced Pt(II)–Pt(IV) polarization of the Pt(III) dimeric unit caused by the electron withdrawal of the equatorial halide ligands. The density functional theory calculation clearly shows that the Pt···Pt interactions between the dimers and the monomer are made by the electron transfer from the monomer to the dimers. The pentanuclear complexes have flexible Pt backbones with the Pt chain adopting either arch or sigmoid structures depending on the crystal packing.

Introduction

One-dimensional transition metal complexes having metal−metal backbones in a long or infinite range are one of the recent research targets of utmost interest. Such complexes are expected to exhibit unusual optical, magnetic, and conducting properties associated with the one-dimensional small domain size or quantum dots.[1] Several one-dimensional metal complexes having appreciable metal−metal interactions have been reported; however, the metal−metal interaction is still limited and compounds with more intensitive metal−metal interactions are extensively searched. In an approach to make one-dimensional oligomers, metal atoms are positioned in a linear array by use of carefully designed template ligands, such as oligo-α-pyridylamino ligands.[2,3] In this case, the number of the available coordination sites of the ligand determines the length of the metal−metal chain. Another approach for formation of metal−metal chains involves oxidation condensation of dinuclear complexes containing d^8 square-planar metal centers or reduction of d^7 metal compounds to form longer metal chain complexes, such as platinum,[4,5] rhodium,[6] and iridium blues.[6] The latter method recently extended the chain length to infinity, and allowed the isolation of rare rhodium[7] and platinum one-dimensional mixed-valence compounds.[8] One-dimensional

* E-mail: kmatsu@waseda.jp.

(1) Bera, J. K.; Dunbar, K. R. *Angew. Chem., Int. Ed.* **2002**, *41*, 4453 and references therein.

(2) (a) Berry, J. F.; Cotton, F. A.; Fewox, C. S.; Lu, T.; Murillo, C. A.; Wang, X. *Dalton Trans.* **2004**, 2297. (b) Lin, S.-Y.; Chen, I.-W. P.; Chen, C.-H.; Hsieh, M.-H.; Yeh, C.-Y.; Lin, T.-W.; Chen, Y.-H.; Peng, S.-M. *J. Phys. Chem. B* **2004**, *108*, 959. (c) Berry, J. F.; Cotton, F. A.; Lei, P.; Lu, T.; Murillo, C. A. *Inorg. Chem.* **2003**, *42*, 3534.

(3) (a) Goto, E.; Begum, R. A.; Zhan, S.; Tanase, T.; Tanigaki, K.; Sakai, K. *Angew. Chem., Int. Ed.* **2004**, *43*, 5029. (b) Murahashi, T.; Mochizuki, E.; Kai, Y.; Kurosawa, H. *J. Am. Chem. Soc.* **1999**, *121*, 10660. (c) Murahashi, T.; Nagai, T.; Mino, Y.; Mochizuki, E.; Kai, Y.; Kurosawa, H. *J. Am. Chem. Soc.* **2001**, *123*, 6927. (d) Osukui, B.; Sheldrick, W. S. *Eur. J. Inorg. Chem.* **1999**, 1325. (e) Osukui, B.; Mintert, M.; Sheldrick, W. S. *Inorg. Chim. Acta* **1999**, *287*, 72.

(4) (a) Barton, J. K.; Rabinowitz, H. N.; Szalda, D. J.; Lippard, S. J. *J. Am. Chem. Soc.* **1977**, *99*, 2827. (b) Matsumoto, K. In *Chemistry and Biochemistry of a Leading Anticancer Drug*; Lippert, B., Ed.; Wiley-VCH: New York, 1999; p 455 (c). Matsumoto, K.; Sakai, K. *Adv. Inorg. Chem.* **1999**, *49*, 375 and references therein.

(5) (a) Sakai, K.; Matsumoto, K. *J. Am. Chem. Soc.* **1989**, *111*, 3074. (b) Sakai, K.; Matsumoto, K.; Nishio, K. *Chem. Lett.* **1991**, 1081. (c) Matsumoto, K.; Sakai, K.; Nishio, K.; Tokisue, Y.; Ito, R.; Nishide, T.; Shichi, Y. *J. Am. Chem. Soc.* **1992**, *114*, 8110.

(6) (a) Tejel, C.; Ciriano, M. A.; Villarroya, B. E.; López, J. A.; Lahoz, F. J.; Oro, L. A. *Angew. Chem., Int. Ed.* **2003**, *42*, 530. (b) Tejel, C.; Ciriano, M. A.; Oro, L. A. *Chem. Eur. J.* **1999**, *5*, 1131 and references therein.

10.1021/ic050942a CCC: $30.25
Published on Web 10/11/2005

Scheme 1

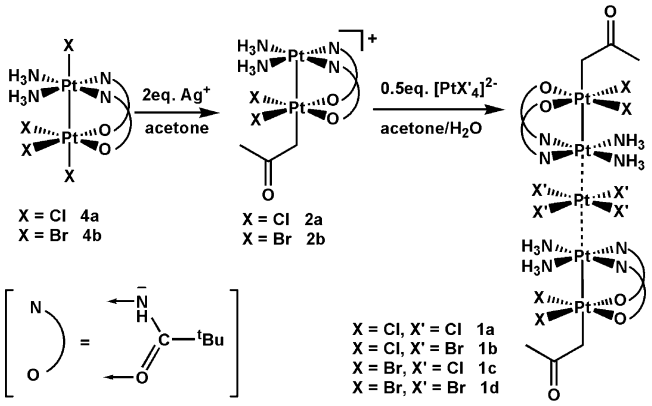

infinite platinum chain compounds, such as Magnus' green salt,[9] are another long-known class of compounds, and rely on the self-stacking of square-planar complexes. We report a method different from these approaches in the present paper: novel Pt pentanuclear chain complexes having Pt−Pt···Pt···Pt−Pt structures with metal−metal bonds. The complexes are Pt(II,III) mixed-valent compounds having acetonyl axial ligands at both ends, $\{[Pt_2(NH_3)_2X_2((CH_3)_3CCONH)_2(CH_2COCH_3)]_2[PtX'_4]\}\cdot n CH_3COCH_3$ (X = X′ = Cl, $n = 2$ (**1a**), X = Cl, X′ = Br, $n = 1$ (**1b**), X = Br, X′ = Cl, $n = 2$ (**1c**), X = X′ = Br, $n = 1$ (**1d**)), which were obtained from the reaction of the pivalamidate-bridged Pt(III) dinuclear complexes having equatorial halide and axial acetonyl ligands, $[Pt_2(NH_3)_2X_2((CH_3)_3CCONH)_2(CH_2COCH_3)]$-X″ (X = Cl (**2a**), Br (**2b**), X″ = NO_3^-, $CH_3C_6H_4SO_3^-$, BF_4^-, PF_6^-, ClO_4^-), with $K_2[PtX'_4]$ (X′ = Cl, Br) (Scheme 1). Complexes **1a**−**1d** have strong Pt(III)···Pt(II) interactions between the Pt(III) dinuclear and $[PtX'_4]^{2-}$ moieties, which are maintained even in solution. In the reactions, the Pt···Pt interactions are made without oxidation or reduction, and constitute a new class of synthetic approach. The density functional theory (DFT) calculation clearly shows how the Pt−Pt interactions are made between the Pt(III) dimers and the Pt(II) monomer.

Experimental Section

Materials and Methods. All reactions and manipulations were performed in air. Solvents were used directly as received. All reagents were purchased from commercial sources and used as received; *cis*-$[Pt(NH_3)_2((CH_3)_3CCONH)_2]\cdot 2H_2O$ (**3**) was prepared as reported.[10]

Elemental analyses were carried out on a Perkin-Elmer PE 2400II. The ^{1}H NMR spectra were recorded on a JEOL Lambda 270 spectrometer and a Bruker AVANCE 400 spectrometer operating at 270 and 400 MHz for ^{1}H, respectively. The ^{195}Pt{^{1}H} NMR spectra were recorded on a JEOL Lambda 500 spectrometer operating at 107.3 MHz for ^{195}Pt. Chemical shifts are in δ unit (parts per million, ppm) referenced to $(CD_3)_2CO$ at 2.04 ppm for ^{1}H and to $H_2[PtCl_6]$ (external reference, 0 ppm) and $K_2[PtCl_4]$ (external reference, −1622 ppm) for ^{195}Pt. The mass spectra were measured on a JEOL JMS-SX102A spectrometer (FAB) and Thermo Quest LCQ-Deca spectrometer (ESI).

Preparation of $\{[Pt_2(NH_3)_2Cl_2((CH_3)_3CCONH)_2(CH_2COCH_3)]_2[PtCl_4]\}\cdot 2CH_3COCH_3$ (1a). A solution of **2a** (0.01 mmol) in 0.9 mL of acetone was added into an aqueous solution of $K_2[PtCl_4]$ (4.22 mg, 0.01 mmol in 0.2 mL of water). The color of the reaction solution immediately changed from yellow to red. Red−orange crystals were obtained by slow evaporation of acetone in dark. Yield 6.64 mg, 71%. Anal. Calcd for $C_{32}H_{74}N_8Cl_8O_8Pt_5$: C 19.63; H 3.81; N 5.72. Found: C 19.66; H 3.37; N 5.30. ^{1}H NMR (400 MHz, acetone-d_6, 23 °C): $\delta = 5.22$ (s, ^2J(Pt,H) = 39.9 Hz, 4H; CH_2), 2.23 (s, 6H; CH_3), 1.16 (s, 36H; CH_3). FAB-MS (positive) 1843.4 (molecule + H^+).

Preparation of $\{[Pt_2(NH_3)_2Cl_2((CH_3)_3CCONH)_2(CH_2COCH_3)]_2[PtCl_4]\}\cdot H_2O$ (1a′). A mixture of **3** (46.62 mg, 0.10 mmol) and $K_2[PtCl_4]$ (41.54 mg, 0.10 mmol) in 1.0 mL of 1 M 1H HNO_3 was added into 2.0 mL of acetone. The mixture was stirred overnight in the dark. After filtration, red crystals were obtained by slow evaporation of acetone in the dark. Yield 15.2 mg, 17%. Anal. Calcd for $C_{26}H_{64}N_8Cl_8O_7Pt_5$: C 16.79; H 3.47; N 6.02. Found: C 16.63; H 3.54; N 5.97. FAB-MS (positive) 1843.1 (molecule + H^+).

Preparation of $\{[Pt_2(NH_3)_2Cl_2((CH_3)_3CCONH)_2(CH_2COCH_3)]_2[PtBr_4]\}\cdot CH_3COCH_3$ (1b). Complex **1b** was prepared in the same way as **1a** by the reaction of **2a** with $K_2[PtBr_4]$ (6.36 mg, 0.01 mmol), and was obtained as orange crystals. Yield 4.87 mg, 50%. Anal. Calcd for $C_{29}H_{68}N_8Br_4Cl_4O_7Pt_5$: C 16.76; H 3.30; N 5.39. Found: C 16.29; H 2.87; N 5.12. ^{1}H NMR (400 MHz, acetone-d_6, 23 °C): $\delta = 5.25$ (s, 4H; CH_2), 2.23 (s, 6H; CH_3), 1.18 (s, 36H; CH_3). FAB-MS (positive) 2020.1 (molecule + H^+).

Preparation of $\{[Pt_2(NH_3)_2Br_2((CH_3)_3CCONH)_2(CH_2COCH_3)]_2[PtCl_4]\}\cdot 2CH_3COCH_3$ (1c). Complex **1c** was prepared in the same way as **1a** by the reaction of **2b** with $K_2[PtCl_4]$ (4.22 mg, 0.01 mmol), and was obtained as red crystals. Yield 5.39 mg, 53%. Anal. Calcd for $C_{32}H_{74}N_8Br_4Cl_4O_8Pt_5$: C 18.00; H 3.49; N 5.25. Found: C 18.04; H 3.47; N 5.10. ^{1}H NMR (400 MHz, acetone-d_6, 23 °C): $\delta = 5.30$ (s, ^2J(Pt,H) = 45.6 Hz, 4H; CH_2), 2.26 (s, 6H; CH_3), 1.18 (s, 36H; CH_3). FAB-MS (positive) 2019.5 (molecule + H^+).

Preparation of $\{[Pt_2(NH_3)_2Br_2((CH_3)_3CCONH)_2(CH_2COCH_3)]_2[PtBr_4]\}\cdot CH_3COCH_3$ (1d). Complex **1d** was prepared in the same way as **1a** by the reaction of **2b** with $K_2[PtBr_4]$ (6.10 mg, 0.01 mmol), and was obtained as orange crystals. Yield 8.25 mg, 75%. Anal. Calcd for $C_{29}H_{68}N_8Br_8O_7Pt_5$: C 16.61; H 3.22; N 4.84. Found: C 16.38; H 2.93; N 4.62. ^{1}H NMR (400 MHz, acetone-d_6, 23 °C): $\delta = 5.32$ (s, 4H; CH_2), 2.29 (s, 6H; CH_3), 1.18(s, 36H; CH_3). FAB-MS (positive) 2197.1 (molecule + H^+).

Preparation of $[Pt_2(NH_3)_2Cl_2((CH_3)_3CCONH)_2(CH_2COCH_3)]$-X″ (X″ = NO_3^-, $CH_3C_6H_4SO_3^-$, BF_4^-, PF_6^-, ClO_4^-) (2a). A suspension of $[Pt_2(NH_3)_2Cl_2((CH_3)_3CCONH)_2Cl_2]$ (**4a**) (7.84 mg, 0.01 mmol) and 2.0 equiv of AgX″ in 0.9 mL of acetone was stirred for 12 h in the dark. After filtration of AgCl, the yellow solution

(7) (a) Finniss, G. M.; Canadell, E.; Campana, C.; Dunbar, K. R. *Angew. Chem., Int. Ed. Engl.* **1996**, *35*, 2772. (b) Prater, M. E.; Pence, L. E.; Clérac, R.; Finniss, G. M.; Campana, C.; Auban-Senzier, P.; Jérome, D.; Canadell, E.; Dunbar, K. R. *J. Am. Chem. Soc.* **1999**, *121*, 8005. (c) Cotton, F. A.; Dikarev, E. V.; Perukhina, M. A. *J. Organomet. Chem.* **2000**, *596*, 130. (d) Cotton, F. A.; Dikarev, E. V.; Perukhina, M. A. *J. Chem. Soc., Dalton Trans.* **2000**, 4241. (e) Pruchnik, F. P.; Jakimowicz, P.; Ciunik, Z.; Stanislawek, K.; Oro, L. A.; Tejel, C.; Ciriano, M. A. *Inorg. Chem. Commun.* **2001**, *4*, 19.

(8) (a) Sakai, K.; Ishigami, E.; Konnno, Y.; Kajiwara, T.; Ito, T. *J. Am. Chem. Soc.* **2002**, *124*, 12088. (b) Sakai, K.; Takeshita, M.; Tanaka, Y.; Ue, T.; Yanagisawa, M.; Kosaka, M.; Tsubomura, T.; Ato, M.; Nakano, T. *J. Am. Chem. Soc.* **1998**, *120*, 11353.

(9) (a) Atoji, M.; Richardson, J. W.; Rundle, R. E. *J. Am. Chem. Soc.* **1957**, *79*, 3017 (b). Miller, J. R. *J. Chem. Soc.* **1965**, 713. (c) Keller, H. J. In *Extended Linear Chain Compounds*; Miller, J. S., Ed.; Plenum Press: New York, 1982; vol. 1, p 357. (d) Bremi, J.; Caseri, W. R.; Smith, P. *J. Mater. Chem.* **2001**, *11*, 2593. (e) Caseri, W. *Platinum Met. Rev.* **2004**, *48*, 91 and references therein.

(10) Chen, W.; Matsumoto, K. *Inorg. Chim. Acta* **2003**, *342*, 88.

Table 1. Crystallographic Data for **1a**−**1d**

	1a·2CH_3COCH_3	**1a′**	**1b**	**1c**·2CH_3COCH_3	**1d**·2CH_3COCH_3
formula	$C_{30}H_{74}N_8Cl_8O_8Pt_5$	$C_{26}H_{62}N_8Cl_8O_6Pt_5$	$C_{26}H_{62}N_8Br_4Cl_4O_6Pt_5$	$C_{30}H_{74}N_8Br_4Cl_4O_8Pt_5$	$C_{30}H_{74}N_8Br_8O_8Pt_5$
M_r	1958.04	1877.92	2019.73	2135.88	2313.72
cryst syst	orthorhombic	monoclinic	monoclinic	orthorhombic	monoclinic
space group	$Pca2_1$	$P2_1/c$	$P2_1/c$	$Pca2_1$	$P2_1/c$
a (Å)	24.395(16)	13.052(5)	11.838(6)	24.607(9)	11.298(2)
b (Å)	15.425(11)	12.092(5)	11.120(5)	15.454(6)	23.321(5)
c (Å)	15.577(10)	15.990(7)	20.017(9)	15.572(6)	11.180(2)
β (deg)		97.635(5)	104.014(8)		92.146(2)
V (Å^3)	5862(7)	2501.1(18)	2556(2)	5922(4)	2943.7(10)
Z	4	4	2	4	2
ρ_{calcd} (g cm^{-3})	2.219	2.494	2.624	2.396	2.606
T (K)	296(2)	293(2)	296(2)	293(2)	296(2)
$\mu_{MoK\alpha}$ (mm^{-1})	12.301	14.408	17.008	14.694	17.314
GOF	0.961	0.992	0.895	1.011	1.033
R_1, wR_2	0.0514, 0.0933	0.0296, 0.0620	0.0571, 0.0984	0.0508, 0.1189	0.0373, 0.0891

was evaporated, affording yellow residue. ^{1}H NMR (400 MHz, acetone-d_6, 23 °C): δ = 4.60 (s, 2H; CH_2), 2.08 (s, 3H; CH_3), 1.12(s, 20H; CH_3). ESI-MS (positive) 751.5 (molecule − X″). The compound is too unstable to obtain satisfactory elemental analysis.

Preparation of [$Pt_2(NH_3)_2Br_2((CH_3)_3CCONH)_2(CH_2COCH_3)$]-X″ (X″ = NO_3^-, $CH_3C_6H_4SO_3^-$, BF_4^-, PF_6^-, ClO_4^-) (2b). Complex **2b** was prepared in the same way as **2a** by using [$Pt_2(NH_3)_2Br_2((CH_3)_3CCONH)_2Br_2$] (**4b**). ^{1}H NMR (400 MHz, acetone-d_6, 23 °C): δ = 5.22 (s, ^2J(Pt,H) = 44.0 Hz, 2H; CH_2), 2.23 (s, 3H; CH_3), 1.13(s, 20H; CH_3). ESI-MS (positive) 841.3 (molecule − X″). The compound is too unstable to obtain satisfactory elemental analysis. The structure of **2b** was confirmed by X-ray analysis (see Supporting Information).

Preparation of [$Pt_2(NH_3)_2Cl_2((CH_3)_3CCONH)_2Cl_2$] (4a). A solution of **3**·H_2O[10] (47.1 mg, 0.10 mmol in 1 mL of water) was added into an aqueous solution of $K_2[PtCl_4]$ (41.5 mg, 0.10 mmol in 1 mL of water). The solution immediately changed from red to navy and became turbid. $Na_2S_2O_8$ (47.6 mg, 0.20 mmol) was added into the navy suspension. After the solution was stirred for 3 h at 40 °C, it became red−orange. After filtration, 1 drop of concentrated HCl was added into the solution. Red crystals of **4a** were obtained by gradual evaporation. Yield 22.1 mg, 29%. Anal. Calcd for $C_{10}H_{26}N_4Cl_4O_2Pt_2$: C 15.67; H 3.42; N 7.31. Found: C 15.51; H 3.26; N 7.28.

Preparation of [$Pt_2(NH_3)_2Br_2((CH_3)_3CCONH)_2Br_2$] (4b). The navy suspension was prepared in the same way as **4a** by the reaction of **3**·H_2O[10] with $K_2[PtBr_4]$ (59.4 mg, 0.10 mmol). $Na_2S_2O_8$ (25.0 mg, 0.10 mmol) was added into the navy suspension. The solution was stirred for 16 h at 40 °C, and became red with brown precipitate. The brown powder of **4b** was obtained by filtration. Red crystals of **4b** were obtained by gradual evaporation of the red solution. Yield 81.4 mg, 86%. Anal. Calcd for $C_{10}H_{26}N_4Br_4O_2Pt_2$: C 12.72; H 2.78; N 5.93. Found: C 12.72; H 2.63; N 5.83.

X-ray Structure Determination. The data were collected on a Bruker SMART 1000 CCD diffractometer. The cell parameters were determined by using the programs SMART[11] and R-LATT.[12] The data reduction and integration were performed with the software package SAINT,[13] whereas the absorption collection was applied by using the program SADABS.[14] The structures were solved by full-matrix least-squares on F^2, and were refined with SHELXTL.[15] Hydrogen atoms were added in the idealized positions. Non-hydrogen atoms were refined with anisotropic temperature parameters. The crystal data are given in Tables 1 and 2. The acetone solvent of **1b** was not found in the X-ray structure but its presence was confirmed by elemental analysis and ^{1}H NMR spectroscopy. The full X-ray data are contained as CCDC-259445 (**1a**), CCDC-259440 (**1a′**), CCDC-259446 (**1b**), CCDC-259442 (**1c**), CCDC-259443 (**1d**), CCDC-259441 (**4a**), and CCDC-259444 (**4b**) in the Supporting Information. These data can also be obtained free of charge via www.ccdc.cam.ac.uk/conts/retrieving.html (or from the Cambridge Crystallographic Data Centre, 12 Union Road, Cambridge CB21EZ, UK; fax: (+44)1223-336-033; or deposit@ccdc.ca.ac.uk).

Table 2. Crystallographic Data for **4a** and **4b**

	4a	**4b**
formula	$C_{10}H_{26}N_4Cl_4O_2Pt_2$	$C_{10}H_{26}N_4Br_4O_2Pt_2$
M_r	766.33	944.17
cryst syst	monoclinic	monoclinic
space group	$P2_1/c$	$P2_1/c$
a (Å)	13.184(5)	13.250(3)
b (Å)	11.263(4)	11.313(2)
c (Å)	15.025(6)	15.613(3)
β (deg)	102.117(7)	104.137(4)
V (Å^3)	2181.4(15)	2269.6(8)
Z	4	4
ρ_{calcd} (g cm^{-3})	2.333	2.763
T (K)	298(2)	298(2)
$\mu_{MoK\alpha}$ (mm^{-1})	13.310	19.365
GOF	1.000	0.918
R_1, wR_2	0.0471, 0.1157	0.0533, 0.1073

Computational Section. DFT calculations using B3LYP functional,[16] which comprises the Hartree−Fock (exact) exchange, the Slater exchange,[17] the Becke (B88) exchange,[18] the Vosco−Wilk−Nusair (VWN) correlation,[19] and the Lee−Yang−Parr (LYP) correlation[20] functionals, were performed to examine the Pt−Pt interaction in **1a**−**1d**. Correlation-consistent polarization plus valence double-ζ (cc-pVDZ) sets of Dunning[21] were used for H, C, N, O, Cl, and Br. For Pt, core electrons were represented by effective core potential of Christiansen et al.,[22] and 5s, 5p, 5d, and

(11) *SMART for WindowsNT/2000, Version 5.625*; Bruker Advanced X-ray Solutions, Inc.: Madison, WI, 2001.
(12) *R-LATT, Reciprocal Lattice Viewer, Version 3.0*; Bruker Advanced X-ray Solutions, Inc.: Madison, WI, 2000.
(13) *SAINT, Data Reduction Software, Version 6.22*; Bruker Advanced X-ray Solutions, Inc.: Madison, WI, 2001.
(14) *SADABS, Area Detector Absorption and other Corrections Software, Version 2.03*; Bruker Advanced X-ray Solutions, Inc.: Madison, WI, 2000.
(15) Sheldrick, G. M. *SHELXTL, Version 5.1*; Bruker Advanced X-ray Solutions, Inc.: Madison, WI, 1998.
(16) (a) Becke, A. D. *J. Chem. Phys.* **1993**, *98*, 5648. (b) Stephens, P. J.; Devlin, F. J.; Chabalowski, C. F.; Frisch, M. J. *J. Phys. Chem.* **1994**, *98*, 11623.
(17) Slater, J. C. *Phys. Rev.* **1951**, *81*, 385.
(18) Becke, A. D. *Phys. Rev. A* **1988**, *38*, 3098.
(19) Vosko, S. H.; Wilk, L.; Nusair, M. *Can. J. Phys.* **1980**, *58*, 1200.
(20) Lee, C.; Yang, W.; Parr, R. G. *Phys. Rev. B* **1988**, *37*, 785.
(21) Dunning, T. H., Jr. *J. Chem. Phys.* **1989**, *90*, 1007.

Scheme 2

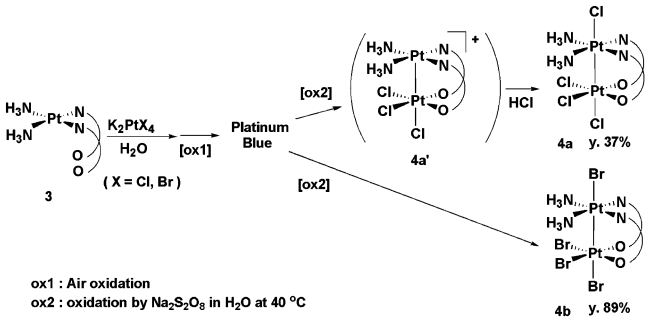

6s valence electrons were represented by (10s5p4d)/(4s3p2d) basis functions. The structural parameters of the complexes **1a**−**1d** were set to their X-ray values. Geometries of the fragments **2a**, **2b**, and $[PtX'_4]^{2-}$ (X′ = Cl, Br) were fixed at those in **1a**−**1d**. While Pt chains in **1a**−**1d** were not exactly linear but quasi-linear, Pt2 and Pt4 were situated on the *z*-axis. Solvent effects were evaluated by means of the conductor polarizable continuum model (CPCM),[23] in which a dielectric constant of 20.7 was adopted for the acetone solvent. The natural population analysis[24] was performed to determine the charge distributions. All calculations were carried out with the use of the Gaussian 03 program.[25]

Results and Discussion

Synthesis. The pivalamidate-bridged Pt(III) dinuclear complexes having axial and equatorial halide ligands $[Pt_2(NH_3)_2X_2((CH_3)_3CCONH)_2X_2]$ (X = Cl (**4a**), Br (**4b**)) were synthesized from *cis*-$Pt(NH_3)_2((CH_3)_3CCONH)_2$ (**3**)[10] as shown in Scheme 2. The synthesis proceeds via formation of a dark blue compound. Unfortunately, the structure of this dark blue compound could not be determined because of the poor crystallinity, though the ESI and FAB MS spectra clearly showed formation of the monocationic Pt(II,III) tetranuclear complex $[Pt_2(NH_3)_2(C_5H_{10}NO)_2X_2]_2]^+$.[4] The dark blue compound was oxidized to red−orange $[Pt_2(NH_3)_2(C_5H_{10}NO)_2Cl_3]^+$ (**4a′**) by $Na_2S_2O_8$ in water. Formation of **4a′** (*m*/*z* 731.5) was confirmed by the ESI MS spectrum of the red−orange solution. Complex **4a** was obtained as red crystals by addition of concentrated HCl to the red−orange solution of **4a′**. Complex **4b** was directly obtained as brown powder by oxidation of the dark blue compound, but formation of $[Pt_2(NH_3)_2(C_5H_{10}NO)_2Br_3]^+$ (**4b′**) (*m*/*z* 862.9) similar to **4a′** was also observed in the ESI MS spectrum of the reaction solution. Complexes **4a** and **4b** are insoluble in H_2O, and therefore are definitely different from the water soluble **4a′** and **4b′**. Although the latter two compounds could not be isolated, the FAB MS spectrum of **4a** shows the presence of **4a′** as well. The release of the Cl ligand in **4a′** would be from the $Pt(N_4)$ atom (the element in parentheses is the coordinating atom), because the $Pt(N_4)$−Cl bond distance is the longest Pt−Cl in **4a** (vide infra). Complexes **4b** and **4b′** also show similar tendency in the Pt−X distances. The attempt to prepare $[Pt_2(NH_3)_2(C_5H_{10}NO)_2I_4]$ and $[Pt_2(NH_3)_2(C_5H_{10}NO)_2I_3]^+$ in a similar manner gave only tar and I_2 vapor.

Yellow complexes **2a** and **2b** were prepared by addition of AgX″ (X″ = NO_3^-, $CH_3C_6H_4SO_3^-$, BF_4^-, PF_6^-, ClO_4^-) to **4a** and **4b** in acetone, respectively. Complexes **2a** and **2b** are reduced to the corresponding Pt(II) dimer compounds $[Pt_2(NH_3)_2X_2((CH_3)_3CCONH)_2]$ by room light (vide infra), and the reducibility of **2a** and **2b** is changed by their counteranions. The reduction proceeds in the order ClO_4^- > BF_4^- > PF_6^- > $CH_3C_6H_4SO_3^-$ > NO_3^-. Yellow crystals of **2b** were obtained, although with poor quality, and the X-ray structure shows the expected structure (see Supporting Information).

Complex **2a** is unstable in solution, and gives $[PtCl_4]^{2-}$ after decomposition. The red crystals of **1a** were obtained after repeated recrystallization of **2a**. Because of the decomposition of **2a**, **1a** is formed from **4a** and Ag^+ in acetone, even without addition of $K_2[PtCl_4]$. The analogous bromide complex **2b** is more stable, but yet it slowly decomposes and gives **1d**. Because of the instability, only poor crystals of **2b** were obtained, but **2a** could not be crystallized. Pentanuclear linear chain Pt(II,III) complexes **1a**−**1d** were synthesized from the reaction of 2 equiv of **2a** or **2b** with 1 equiv of $K_2[PtX'_4]$ (X′ = Cl, Br). The ^{1}H NMR spectra of the reaction solutions indicate that the reactions proceeded almost quantitatively, however for crystallization, excess $K_2[PtX'_4]$ gives better yield. The FAB MS spectra of **1a**−**1d** show the presence of molecular ions of **1a**−**1d**. Usually weak bonds such as ionic bonds are fragmented in FAB MS measurement, and so the Pt···Pt interactions between the dinuclear and mononuclear units seem to be substantially stable. Similar pentanuclear complex was not formed when $K_2[PtX'_4]$ was reacted with the analogous compound of **2a** and **2b**, i.e., $[Pt_2(NH_3)_4((CH_3)_3CCONH)_2(CH_2COCH_3)]^{3+}$ (**5**)[26a] having equatorial ammine ligands. The DFT calculation clearly shows how the Pt···Pt interactions are strengthened and how the equatorial halide ligands are important to such pentanuclear chain compounds (vide infra).

Crystal Structures. The X-ray structure of **4a** is shown in Figure 1. The structural parameters of **4a** and **4b** show that the axial Pt−X bonds are significantly longer than the equatorial ones (Table 3). Similar difference of Pt−X bond lengths between axial and equatorial ligands is also reported in the 1-methyluracilato- and 1-ethylthyminato-bridged Pt(III) dinuclear complexes having axial and equatorial

(22) Ross, R. B.; Powers, J. M.; Atashroo, T.; Ermler, W. C.; LaJohn, L. A.; Christiansen, P. A. *J. Chem. Phys.* **1990**, *93*, 6654.
(23) Barone, V.; Cossi, M. *J. Phys. Chem. A* **1998**, *102*, 1995.
(24) Reed, A. E.; Weinstock, R. B.; Weinhold, F. J. *J. Chem. Phys.* **1985**, *83*, 735.
(25) Frisch, M. J.; Trucks, G. W.; Schlegel, H. B.; Scuseria, G. E.; Robb, M. A.; Cheeseman, J. R.; Montgomery, J. A., Jr.; Vreven, T.; Kudin, K. N.; Burant, J. C.; Millam, J. M.; Iyengar, S. S.; Tomasi, J.; Barone, V.; Mennucci, B.; Cossi, M.; Scalmani, G.; Rega, N.; Petersson, G. A.; Nakatsuji, H.; Hada, M.; Ehara, M.; Toyota, K.; Fukuda, R.; Hasegawa, J.; Ishida, M.; Nakajima, T.; Honda, Y.; Kitao, O.; Nakai, H.; Klene, M.; Li, X.; Knox, J. E.; Hratchian, H. P.; Cross, J. B.; Bakken, V.; Adamo, C.; Jaramillo, J.; Gomperts, R.; Stratmann, R. E.; Yazyev, O.; Austin, A. J.; Cammi, R.; Pomelli, C.; Ochterski, J. W.; Ayala, P. Y.; Morokuma, K.; Voth, G. A.; Salvador, P.; Dannenberg, J. J.; Zakrzewski, V. G.; Dapprich, S.; Daniels, A. D.; Strain, M. C.; Farkas, O.; Malick, D. K.; Rabuck, A. D.; Raghavachari, K.; Foresman, J. B.; Ortiz, J. V.; Cui, Q.; Baboul, A. G.; Clifford, S.; Cioslowski, J.; Stefanov, B. B.; Liu, G.; Liashenko, A.; Piskorz, P.; Komaromi, I.; Martin, R. L.; Fox, D. J.; Keith, T.; Al-Laham, M. A.; Peng, C. Y.; Nanayakkara, A.; Challacombe, M.; Gill, P. M. W.; Johnson, B.; Chen, W.; Wong, M. W.; Gonzalez, C.; Pople, J. A. *Gaussian 03*, revision C.02; Gaussian, Inc.: Wallingford, CT, 2004.

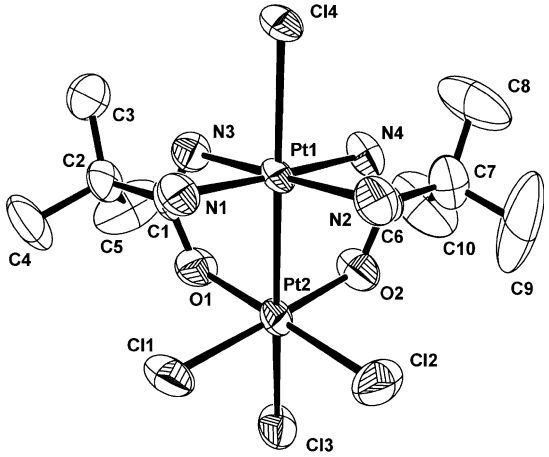

Figure 1. Structure of complex **4a**.

Table 3. Selected Structural Parameters of **4a**, **4b**, and **6**

	4a (X = Cl)	**4b** (X = Br)	**6** (X = Cl)
	Bond Distances (Å)		
Pt1−Pt2	2.6184(9)	2.6200(9)	2.6068(7)
Pt1−X4	2.445(3)	2.5748(19)	2.460(3)
Pt2−X1	2.299(3)	2.403(2)	
Pt2−X2	2.292(3)	2.418(2)	
Pt2−X3	2.400(3)	2.5304(19)	2.399(4)
	Bond Angles (deg)		
X3−Pt2−Pt1	172.48(9)	171.47(6)	172.31(8)
X4−Pt1−Pt2	167.67(7)	166.55(6)	173.68(13)

chloride ligands.[27] Comparison of the structures of **4a** with analogous compound $[Pt_2(NH_3)_4((CH_3)_3CCONH)_2Cl_2]^{2+}$ (**6**) having equatorial ammine ligands shows that the Pt−Pt distance is longer for **4a** (2.6184(9) Å in **4a** and 2.6068(7) Å in **6** (see Supporting Information)). We have already suggested that the Pt(III)−Pt(III) bond is polarized to Pt(IV)−Pt(II) to a various extent depending on the axial ligands,[26] but the above comparison shows that the equatorial ligand also affects the Pt−Pt polarization, i.e., the large electronegativity of the equatorial chloride ligands induces $Pt(IV)(Cl_2O_2)-Pt(II)(N_4)$ polarization and probably this makes **4a** less stable than **4b**.

Comparison of the Pt−Pt distances of **2b** (see Supporting Information) with **5**[26a] (2.665(3)−2.701(2) Å in **2b** and 2.6892(6) Å in **5**[26a]) does not clearly show that the equatorial ligand affects the Pt−Pt polarization, since the crystal of **2b** was of poor quality and the Pt−Pt distances have ranged widely. However, complex **2b** has vacant axial site opposite to the acetonyl ligand, whereas **5** has a nitrate ligand weakly coordinated. This suggests that the Pt−Pt bond in **2b** is more polarized to Pt(IV)−Pt(II) than in **5**.

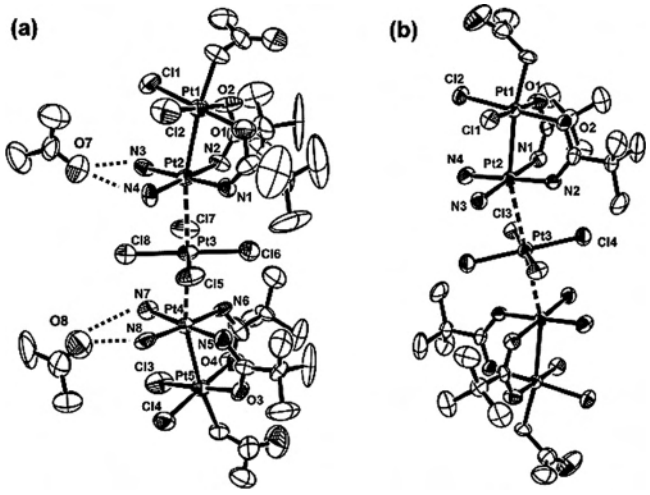

Figure 2. Crystal structures of the arch Pt backbone complex (**1a**) and the sigmoid Pt backbone complex (**1a′**): (a) $\{[Pt_2(NH_3)_2Cl_2((CH_3)_3CCONH)_2(CH_2COCH_3)]_2[PtCl_4]\}\cdot 2CH_3COCH_3$ (**1a**), (b) $\{[Pt_2(NH_3)_2Cl_2((CH_3)_3CCONH)_2(CH_2COCH_3)]_2[PtCl_4]\}\cdot H_2O$ (**1a′**). H atoms are omitted for clarity.

Furthermore, the Pt−Pt distances of the dimer units in **1a**−**1d** are longer than that of compound **5**[26a] having equatorial ammine ligands (2.6901(9)−2.7146(14) Å in **1a**−**1d** (Table 4) and 2.6892(6) Å in **5**[26a]). This suggests that the Pt−Pt bonds in **1a**−**1d** are more polarized to Pt(IV)−Pt(II) than in **5**. All these facts suggest that the equatorial halide ligands induce polarization of the Pt−Pt bond.

The X-ray structure of **1a** is shown in Figure 2. The structural parameters of **1a**−**1d** are listed in Table 4. The pentanuclear structure is approximated as consisting of two cationic amidate-bridged Pt(III) dimers and a $[PtX'_4]^{2-}$ anion. The interaction between the dimer and the monomer moieties resembles the interaction of $[PtCl_4]^{2-}$ and $[Pt(NH_3)_4]^{2+}$ in Magnus' green salt[9] as discussed later. The Pt chains of **1a**−**1d** are nearly linear (the Pt1−Pt2−Pt3 angles range from 163.461(13) to 167.47(4)°).

The distances of $Pt(N_4)-Pt(X_4)$ in **1a**−**1d** are significantly shorter than the $Pt(N_4)-Pt(Cl_4)$ distance of about 3.24 Å[9] in Magnus' green salt. The Pt oxidation states in **1a**−**1d** are localized approximately to $Pt(III)_2Pt(II)Pt(III)_2$ and are not delocalized as in the Pt(II,III) tetranuclear[4] and octanuclear[5] zigzag chain complexes. The pentanuclear complexes were also synthesized directly from the reaction of complex **3** and $[PtCl_4]^{2-}$ in acetone/1 M HNO_3 at room temperature. The pentanuclear complex obtained with this method $\{[Pt_2(NH_3)_2Cl_2((CH_3)_3CCONH)_2(CH_2COCH_3)]_2[PtCl_4]\}\cdot H_2O$ (**1a′**) has the same formula but a different Pt−Pt backbone structure as shown in Figure 2b and Table 4. The arch Pt backbones in **1a** and **1c** are caused by the hydrogen bonds between the ammine ligands and acetone molecules in the lattice (O7···N3(**1a**) 3.026 Å, O7···N4(**1a**) 2.949 Å, O8···N7(**1a**) 3.053 Å, O8···N8(**1a**) 3.190 Å, O8···N3(**1c**) 2.987 Å,

(26) (a) Matsumoto, K.; Matsunami, J.; Mizuno, K.; Uemura, H. *J. Am. Chem. Soc.* **1996**, *118*, 8959. (b) Matsumoto, K.; Ochiai, M. *Coord. Chem. Rev.* **2002**, *231*, 229. (c) Saeki, N.; Nakamura, N.; Ishibashi, T.; Arime, M.; Sekiya, H.; Ishihara, K.; Matsumoto, K. *J. Am. Chem. Soc.* **2003**, *125*, 3605. (d) Ochiai, M.; Lin, Y.-S.; Yamada, J.; Misawa, H.; Arai, S.; Matsumoto, K. *J. Am. Chem. Soc.* **2004**, *126*, 2536. (e) Arime, M.; Ishihara, K.; Matsumoto, K. *Inorg. Chem.* **2004**, *43*, 309. (f) Ochiai, M.; Matsumoto, K. *Chem. Lett.* **2002**, 270. (g) Lin, Y.-S.; Misawa, H.; Yamada, J.; Matsumoto, K. *J. Am. Chem. Soc.* **2001**, *123*, 569. (h) Lin, Y.-S.; Takeda, S.; Matsumoto, K. *Organometallics* **1999**, *18*, 4897. (i) Matsumoto, K.; Nagai, Y.; Matsunami, J.; Mizuno, K.; Abe, T.; Somazawa, R.; Kinoshita, J.; Shimura, H. *J. Am. Chem. Soc.* **1998**, *120*, 2900.

(27) (a) Peilert, M.; Weissbach, S.; Freisinger, E.; Korsunsky, V. I.; Lippert, B. *Inorg. Chim. Acta* **1997**, *265*, 187. (b) Micklitz, W.; Renn, O.; Schöllhorn, H.; Thewalt, U.; Lippert, B. *Inorg. Chem.* **1990**, *29*, 1836. (c) Renn, O.; Albinati, A.; Lippert, B. *Angew. Chem., Int. Ed. Engl.* **1990**, *29*, 84. (d) Lippert, B.; Schöllhorn, H.; Thewalt, U. *Inorg. Chem.* **1986**, *25*, 407. (e) Zangrando, E.; Pichierri, F.; Randaccio, L.; Lippert, B. *Coord. Chem. Rev.* **1996**, *156*, 275.

Table 4. Selected Structural Parameters of **1a**−**1d**[a]

	1a	1a′	1b	1c	1d
			Bond Distances (Å)		
Pt1−Pt2	2.6986(18)	2.6901(9)	2.7146(14)	2.7023(12)	2.7134(6)
Pt2−Pt3	3.014(2)	3.0054(11)	3.1109(15)	3.0237(13)	3.1039(5)
Pt1−X1	2.319(6)	2.296(2)	2.313(5)	2.416(3)	2.4156(11)
Pt1−X2	2.283(6)	2.302(2)	2.305(6)	2.404(2)	2.4165(11)
Pt1−C_{axial}	2.09(2)	2.099(8)	2.05(2)	2.113(18)	2.096(8)
Pt3−X_{av}	2.313(6)	2.312(3)	2.452(2)	2.315(5)	2.4421(12)
			Bond Angles (deg)		
Pt1−Pt2−Pt3	167.47(4)	163.666(15)	165.79(3)	166.43(3)	163.461(13)
form[b]	A	S	S	A	S

[a] Parameters for Pt4 and Pt5 are close to those of Pt1 and Pt2, and therefore are omitted. [b] Pt backbone: arch (A), sigmoid (S).

Scheme 3

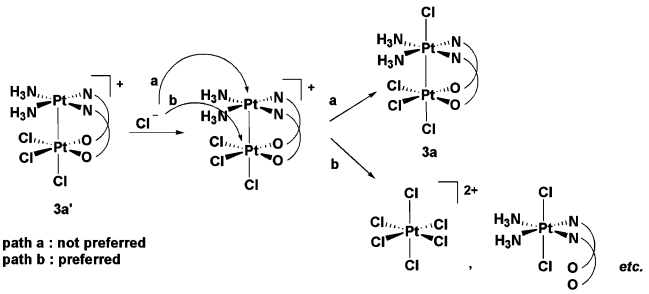

O8···N4(**1c**) 2.979 Å).[28] No such hydrogen bonding is observed for the sigmoidal Pt backbone compounds in Table 4.

Polarization of the Pt−Pt Bonds. We mentioned above that the large electronegativity of the equatorial chloride ligands induces Pt(IV)(Cl_2O_2)−Pt(II)(N_4) polarization, which led to the instability and poor yield of **4a**. Complex **4a** is formed by addition of concentrated HCl to **4a′** (vide supra), but Cl^- actually tends more to attack at Pt(Cl_3O_2). Therefore **4a′** easily decomposes to the corresponding monomeric Pt(IV) compounds as shown in Scheme 3. Since the solution is strongly acidic, all the decomposed monomeric compounds are obtained as Pt(IV) compounds. Complex **4a′** rapidly decomposes, and **4a** is formed only in the presence of concentrated HCl. It is known that the Pt(III)−Pt(III) bond is stabilized only in strongly acidic condition.[4] When KCl is added instead of concentrated HCl, **4a′** totally decomposes to monomeric complexes, and **4a** is not obtained. Both monomeric compounds were identified with X-ray structure determination. Similar decomposition was difficult for **4b**, because it is hard for Br^- to attack Pt(Br_3O_2) due to the lower polarization of the Pt−Pt bond. The larger atomic radius of bromide compared to Cl^- also prevents decomposition of **4b**.

The comparison of the ^{195}Pt{^{1}H} NMR chemical shifts of **2a** and those of the analogous compound **5**[26a] (Table 5) also shows that the equatorial chloride ligands cause more polarization in the Pt−Pt bond, i.e., the bond in **2a** is closer to Pt(II)(N_4)−Pt(IV)(Cl_2O_2) more than that of **5**, since the signal of Pt(Cl_2O_2) in **2a** is shifted to a lower field than that of Pt(N_2O_2) in **5**, whereas the value of Pt(N_4) in **2a** is in a higher field than that of **5**.[26] Such pronounced polarization in **2a** is caused by the electron withdrawal of the equatorial halide ligands, leaving the chloride coordinated Pt atom close to Pt(IV). Most notably, the pentanuclear compounds are not formed when **5** instead of **2a** or **2b** is reacted with $[PtX'_4]^{2-}$ (vide supra). It seems that the nearly Pt(II) oxidation state of Pt(N_4) in **2a** and **2b** is essential to stabalize the Pt···Pt interaction between the dimer and monomer units in **1a**−**1d** as in Magnus' green salt.[9] The chemical shifts and the ^1J(Pt−Pt) couplings of **1a** and **1d** show that the pentanuclear structures are retained in the solution. Pentanuclear complexes containing two dinuclear units and a mononuclear unit like **1a**−**1d** have been reported for Au(II)−Au(II)−Au(I)−Au(II)−Au(II),[29] in which Au−Au bonds between the dimer and the monomer units seem to be caused by similar polarization of the dimer unit.

Due to the pronounced Pt(II)−Pt(IV) polarization, compounds **1a**, **2a**, and **2b** release both acetone and hydroxyacetone gradually in D_2O, and **2a** and **2b** are reduced to the corresponding Pt(II) dimer compounds. Compound **1a** is reduced to the Pt(II) dimer and the monomer. This should be compared to **5**,[26a] which undergoes nucleophilic attack of water at the α-carbon atom to release only hydroxyacetone.[26a] The reactions of **1a**, **2a**, and **2b** would proceed via a radical process, since compounds **1a**, **2a**, and also **2b** but to a lesser existent, are easily decomposed and reduced to the Pt(II) species by room light. Compound **1d** produces only acetone via electrophilic attack of water. This reactivity corresponds to Pt(IV) alkyl compounds,[30] and strongly supports that the polarization and the electronic state of the Pt−Pt bond are affected and induced by the equatorial halide ligands.

DFT Calculations for Clarification of the Pt···Pt Interaction. DFT calculations were performed to examine the Pt−Pt interaction in **1a**−**1d**. The energy diagram for the formation of **1a** from the two dimer cations $[Pt_2(NH_3)_2Cl_2((CH_3)_3CCONH)_2(CH_2COCH_3)]^+$ and the monomer anion $[PtCl_4]^{2-}$ is shown in Figure 3. The intermediate in Figure 3 corresponds to the trinuclear complex formed from one dimer

(28) Desiraju, G. R.; Steiner, T. *The Weak Hydrogen Bonds in Structural Chemistry and Biology*, International Union of Crystallography Monographs on Crystallography, 9; Oxford University Press: Oxford, 1999; p 13.

(29) (a) Usón, R.; Laguna, A.; Laguna, M.; Jiménez, J.; Jones, P. G. *Angew. Chem., Int. Ed. Engl.* **1991**, *30*, 198. (b) Laguna, A.; Laguna, M.; Jiménez, J.; Lahoz, F. J.; Olmos, E. *Organometallics* **1994**, *13*, 253.

(30) Stahl, S. S.; Labinger, J. A.; Bercaw, J. E. *Angew. Chem., Int. Ed.* **1998**, *37*, 2180 and references therein.

Table 5. The ^{195}Pt NMR Chemical Shifts of the Pentanuclear Complexes, Pt(III) Dimers, and Several Pt(II) Monomers

compounds	coord. atoms	$\delta(^{195}\text{Pt})$ (ppm)	$^1J(^{195}\text{Pt}-^{195}\text{Pt})$ (Hz)
$\{[Pt^{III}_2(NH_3)_2(PVM)_2Cl_2(CH_2COCH_3)]_2[PtCl_4]\}$[a] (**1a**)	Cl_2O_2	268	3154 ($Cl_2O_2-N_4$)
	N_4	−2208	ND (Cl_4-N_4)
	Cl_4	−1888	
$\{[Pt^{III}_2(NH_3)_2(PVM)_2Br_2(CH_2COCH_3)]_2[PtBr_4]\}$[a] (**1d**)	Br_2O_2	−230	3069 ($Br_2O_2-N_4$)
	N_4	−2254	4957 (Br_4-N_4)
	Br_4	−2689	
$[Pt^{III}_2(NH_3)_2(PVM)_2Cl_2(CH_2COCH_3)]X'''$[b] (**2a**)	Cl_2O_2	253	3251
	N_4	−2080	
$[Pt^{III}_2(NH_3)_2(PVM)_2Br_2(CH_2COCH_3)]X'''$[b] (**2b**)	Br_2O_2	−241	3187
	N_4	−2122	
$[Pt^{III}_2(NH_3)_2(PVM)_2Cl_3]^+$[c] (**4a′**)	Cl_2O_2	535	8280
	N_4	−1023	
$[Pt^{III}_2(NH_3)_2(PVM)_2Br_3]^+$[c] (**4b′**)	Br_2O_2	341	7414
	N_4	−1752	
$[Pt^{III}_2(NH_3)_4(PVM)_2Cl_2](NO_3)_2$[d] (**6**)	N_2O_2	8	3608
	N_4	−1190	
$[Pt^{III}_2(NH_3)_4(PVM)_2(CH_2COCH_3)](NO_3)_3$[e] (**5**)	N_2O_2	−100	3477
	N_4	−1892	
$H_2Pt^{IV}Cl_6$[e]	Cl_6	0	
$K_2Pt^{II}Cl_4$[e]	Cl_4	−1623	
$K_2Pt^{II}Br_4$[e]	Br_4	−2672	
cis-$[Pt^{II}(NH_3)_2(PVM)_2]$[e] (**3**)	N_4	−2531	
cis-$[Pt^{IV}(NH_3)_2(PVM)_2Cl_2]$[e,5]	N_4	302	

[a] Measured in acetone-d_6:D_2O = 9:1, and locked with D_2O in an inner tube. [b] Measured in acetone-d_6, and locked with D_2O in an inner tube. [c] Since complexes **4a** and **4b** are insoluble in usual solvents, only the chemical shifts of **4a′** and **4b′** are reported. Complexes **4a′** and **4b′** were prepared in D_2O as shown in Scheme 1. [d] Measured in 0.1 M $DClO_4$. [e] Measured in D_2O (PVM = $(CH_3)_3CCONH$; X‴ = p-$CH_3C_6H_4SO_3^-$, NO_3^-).

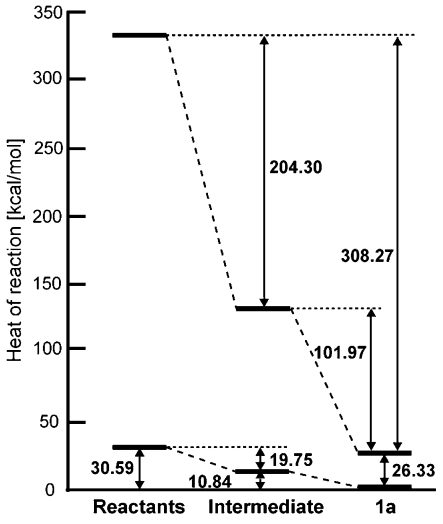

Figure 3. The energy diagram for the formation of **1a** from the two dimer cations $[Pt_2(NH_3)_2Cl_2((CH_3)_3CCONH)_2(CH_2COCH_3)]^+$ and the monomer anion $[PtCl_4]^{2-}$ (reactants). The upper diagram is the result without solvent effect, and the lower with solvent effect. The "intermediate" corresponds to the trinuclear 1:1 dimer and monomer adduct.

and a monomer complex. Without the solvent effect, the heats of reactions in the first and second steps are calculated to be 204.30 and 101.97 kcal/mol, respectively, whereas they are 19.75 and 10.84 kcal/mol with the solvent effect, respectively. Solvent effect is essential to evaluate the heat of reactions in ionic species like in the present case. The total heat of reaction of 30.59 kcal/mol indicates that the averaged bond energy of the present novel Pt(II)−Pt(III) bond between the dimer and monomer is estimated to be 15 kcal/mol. Several bond energies of Pt−Pt bonds reported are 7−22 kcal/mol for Pt(0)−Pt(0),[31] 39−58 kcal/mol for Pt(I)−Pt(I),[32] and 10−47 kcal/mol for Pt(II)−Pt(II).[33] Thus, the present Pt(II)−Pt(III) bond is comparable with or slightly weaker than the Pt(0)−Pt(0) and Pt(II)−Pt(II) bonds, and is much weaker than the Pt(I)−Pt(I) bonds.

(31) Sakaki, S.; Ogawa, M.; Musashi, Y. *J. Phys. Chem.* **1995**, *99*, 17134.

Table 6. Charge Distributions in the Separated (Reactants) and Combined (**1a**) Systems[a]

		charge		
moiety		separated system	combined system	
dimer	Pt1	+1.016	+1.020	(+0.004)
	Pt2	+0.765	+0.738	(−0.027)
	Cl	−0.451	−0.461	(−0.010)
	Cl	−0.441	−0.452	(−0.011)
	NH_3	+0.333	+0.327	(−0.006)
	NH_3	+0.328	+0.323	(−0.005)
	$C_5H_{10}NO$	−0.261	−0.258	(+0.003)
	$C_5H_{10}NO$	−0.253	−0.253	(0.000)
	CH_2COCH_3	−0.036	−0.098	(−0.062)
	subtotal	+1.000	+0.886	(−0.114)
monomer	Pt3	+0.359	+0.349	(−0.010)
	Cl′	−0.588	−0.500	(+0.088)
	Cl′	−0.592	−0.550	(+0.042)
	Cl′	−0.582	−0.522	(+0.060)
	Cl′	−0.597	−0.537	(+0.060)
	subtotal	−2.000	−1.760	(+0.240)
dimer	Pt4	+0.768	+0.740	(−0.028)
	Pt5	+1.030	+1.033	(+0.003)
	Cl	−0.458	−0.470	(−0.012)
	Cl	−0.438	−0.451	(−0.013)
	NH_3	+0.336	+0.331	(−0.005)
	NH_3	+0.338	+0.332	(−0.006)
	$C_5H_{10}NO$	−0.262	−0.260	(+0.002)
	$C_5H_{10}NO$	−0.241	−0.240	(+0.001)
	CH_2COCH_3	−0.073	−0.141	(−0.068)
	subtotal	+1.000	+0.874	(−0.126)

[a] Differences between the two systems are shown in parentheses

The charge distributions in the separated and combined systems of **1a** are shown in Table 6. Since complex **1a** is not exactly symmetric, the charge distributions in the two

Table 7. Orbital Components of the Transferred Electrons for C_{axial}, Pt, and Cl′ Atoms in **1a**[a]

atoms	orbital type	orbital component	atoms	orbital type	orbital component
C_{axial}	s	+0.001	Pt3	s	+0.042
	p_x	+0.005		p	+0.001
	p_y	−0.003		d_{xy}	−0.004
	p_z	+0.036		d_{xz}	−0.004
	d	0.000		d_{yz}	−0.004
				$d_{x^2-y^2}$	+0.065
Pt1	s	−0.001		d_{z^2}	−0.085
	p	−0.002			
	d_{xy}	−0.006	Cl′	s	−0.002
	d_{xz}	+0.004		p_x	−0.005
	d_{yz}	−0.001		p_y	−0.034
	$d_{x^2-y^2}$	0.000		p_z	−0.018
	d_{z^2}	+0.001		d	0.000
Pt2	s	+0.016			
	p	+0.001			
	d_{xy}	+0.016			
	d_{xz}	+0.003			
	d_{yz}	+0.003			
	$d_{x^2-y^2}$	+0.001			
	d_{z^2}	−0.014			

[a] The calculated data for Pt4 and Pt5 are close to those of Pt2 and Pt1, and therefore, are omitted.

dimer moieties are close to each other. In both separated and combined systems, the five Pt atoms are categorized into three groups by the geometry and the charges: (Pt1 and Pt5), (Pt2 and Pt4), and Pt3. The charge density of these groups corresponds to their formal charges +3 in both (Pt1, Pt5) and (Pt2, Pt4), and +2 in Pt3. Furthermore, the calculated results confirm the polarization of the Pt−Pt bonds in the dimer moieties close to Pt(IV) (Pt1, Pt5) and Pt(II) (Pt2, Pt4).

The electron densities of the two dimer moieties increase by 0.114 and 0.126 after **1a** formation, while that of monomer decreases by 0.240 (Table 6). This result indicates that electrons are transferred from the monomer to the dimers on the formation of **1a**. It seems that the main electron flow on the **1a** formation is from the equatorial Cl ligands in the monomer to the axial acetonyl ligands in the dimers, and the electron density changes on the Pt atoms are smaller, i.e., (−0.004, −0.003), (+0.027, +0.028), and +0.010 for (Pt1, Pt5), (Pt2, Pt4), and Pt3, respectively. Even after this electron flow, the dimers and the monomer are still significantly charged, which suggests ionic interaction would exist between the dimers and the monomer.

Orbital components of the transferred electrons are calculated for the axial C, Pt1, Pt2, Pt3, and Cl′ atoms and are shown in Table 7. In the axial C atom, p_z orbital plays a key role to accept electrons. Since the Cl′ atom was located not exactly on the *xy*-plane, electrons are donated not only from the p_y orbital of Cl′ but also from the p_z orbital. Although the Pt1 and Pt2 atoms are in the pathway of the electron transfer from Cl′ to the axial C atom, all of the orbital components in Pt1 and Pt2 are less than 0.016. On the other hand, the s and $d_{x^2-y^2}$ orbitals of Pt3 mainly accept the electrons from Cl′, and the d_{z^2} orbital of Pt3 donates electrons.

(32) Sugimoto, M.; Horiuchi, F.; Sakaki, S. *Chem. Phys. Lett.* **1997**, *274*, 543.
(33) Novoa, J. J.; Aullón, G.; Alemany, P.; Alvarenz, S. *J. Am. Chem. Soc.* **1995**, *117*, 7169.

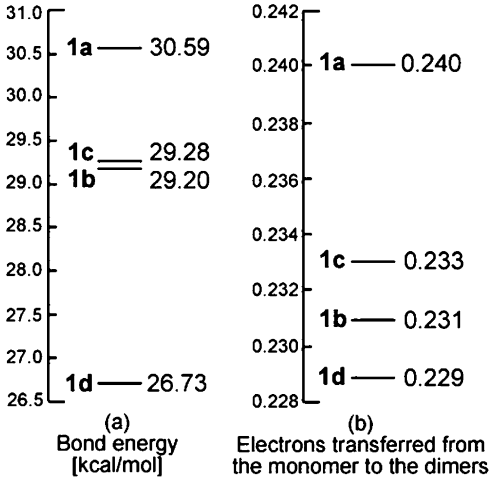

Figure 4. Comparison of the bond energies and the electron transfers from the monomer to the dimers in **1a**−**1d**.

The s and $d_{x^2-y^2}$ orbitals of Pt3 contribute to the Pt3−Cl′ bonds and the d_{z^2} orbital contributes to the Pt3−Pt2 as well as the Pt3−Pt4 bonds.

The electron flow from the monomer to the dimers is also observed in complexes **1b**, **1c**, and **1d**, and the bond energies and the electron transfers in **1a** − **1d** are compared in Figure 4. The bond energy decreases in the order **1a** > **1c** > **1b** > **1d**. The X-ray data in Table 1 indicate that the Pt2−Pt3 distance increases in the order **1a** < **1c** < **1d** < **1b**. The opposite order is observed for the Pt1−C_{axial} distances. The differences in the Pt1−Pt2 distances are comparably small. Consequently, the total distances of the C_{axial}−Pt1−Pt2−Pt3 bonds lie in the order **1a**(7.80 Å) < **1c**(7.839 Å) < **1b**(7.88 Å) < **1d**(7.913 Å). Thus, the C_{axial}−Pt1−Pt2−Pt3 distance is elongated as the bond energy decreases. This order also corresponds to the electron-transfer amount in Figure 4b.

Concluding Remarks. Novel linear pentanuclear complexes having Pt_5 chain backbones have been synthesized from the reaction of the amidate-bridged Pt(III) dimer complexes and $[PtX_4]^{2-}$. The pentanuclear complexes are composed of two molecules of the amidate-bridged Pt(III) dimer complexes sandwiching one molecule of $[PtX_4]^{2-}$. The oxidation states of the chain Pt_5 metals are approximated to Pt(III)−Pt(III)···Pt(II)···Pt(III)−Pt(III), and the strong interactions between Pt(III) and Pt(II) are noteworthy, since there is no bridging ligand.

The DFT calculation clearly shows that the Pt···Pt interactions between the monomer and dimers are made by the electron transfer from the monomer to the dimers. This electron flow finally goes to the terminal axial acetonyl ligands, and the electron densities of the α-carbon atoms are increased. The increased electron density decreases the electrophilicity of the α-carbon atoms, and **1d** releases only acetone in water, though **1a**, **2a**, and **2b** release both acetone and hydroxyacetone. This should be compared to the reactivity of **5**, which releases only hydroxyacetone.[26a] The difference between **1a** and **1d** is explained by the comparison with their orbital components of the transferred electrons for α-carbon atoms in the DFT calculation (vide supra). The

electron density of the α-carbon atoms of **1d** is higher than that of **1a** (+0.039 for **1a** and +0.031 for **1d**), so the electrophilicity of the α-carbon atoms in **1d** is decreased.

Previously amidate-bridged Pt(III) dinuclear complexes having an axial alkyl ligand did not have any ligand at the opposite axial site due to the strong trans influence of the alkyl ligand even via the Pt−Pt bond;[26] however, the present study shows that the vacant axial sites of Pt2 and Pt4 can accept the Pt(II) d_{z^2} electron of Pt3 to make the Pt−Pt bond, when the Pt(III) dimer has equatorial halide ligands. The effect of the equatorial halide ligands on Pt1 and Pt5 is remarkable. The ligands polarize the Pt(III)−Pt(III) bond approximately to Pt(IV)−Pt(II) and induce the electron transfer from even the highly electronegative halide ions on Pt3 to the axial acetonyl ligands via Pt3−Pt2−Pt1 and Pt3−Pt4−Pt5 bonds. This electron transfer elucidates the highly delocalized Pt−Pt interactions along the pentanuclear chains, similar to the previously reported amidate-bridged Pt(III) dinuclear complexes.[26]

Acknowledgment. Financial support from the 21COE "practical Nano-Chemistry" and Nano-COE from MEXT, Japan, are gratefully acknowledged.

Supporting Information Available: Full tables of the data collection parameters, anisotropic temperature factors, and bond distances and angles for **1a**, **1a′**, **1b**, **1c**, **1d**, **4a**, and **4b**. Crystal structures of **1b**, **1c**, **1d**, **2b**, **4b**, and **6** are included. The data obtained by the DFT calculations of **1a**−**1d** are also available. This material is available free of charge via the Internet at http://pubs.acs.org.

IC050942A